

ORIGINAL RESEARCH

A radiomics model derived by combination of radiomics signature and clinical risk factors predict of lymph node metastasis for men renal pelvis urothelial carcinoma

Jingyi Huang¹, Fan Chen¹, Chengcheng Gao², Zhenyu Shu³, Gang Tao^{4,*}

¹Department of Radiology, Zhejiang Medical and Health Group Hangzhou Hospital, 310022 Hangzhou, Zhejiang, China

²Department of Radiology, Hangzhou First People's Hospital, 310006 Hangzhou, Zhejiang, China

³Department of Radiology, Zhejiang Provincial People's Hospital, Affiliated People's Hospital, Hangzhou Medical College, 314408 Hangzhou, Zhejiang, China

⁴Department of Oncology, Zhejiang Medical and Health Group Hangzhou Hospital, 310022 Hangzhou, Zhejiang, China

***Correspondence**

tg@zyjhzyy.com
(Gang Tao)

Abstract

This study aims to propose a radiomics model to identify male patients suffering from renal pelvis urothelial carcinoma (RPUC) with preoperative lymph node (LN) metastasis. In a study involving 133 male RPUC patients, 94 were assigned to a training group and 39 to a testing group. Their arterial-phase computed tomography (CT) images were analyzed to extract radiomics features, which were then refined through data reduction and feature selection. Using the least absolute shrinkage and selection operator (LASSO), a radiomics signature was created, which was then incorporated into a Logistic regression classifier in the training group to predict pathologic lymph node metastases. A comprehensive radiomics model was developed using multivariate logistic regression, integrating clinical risk factors. The model's efficacy was evaluated in both sets using discrimination, calibration and decision curve analyses in both the training and testing sets. The constructed signature, composed of eight promising imaging-derived features, showed strong discrimination ability in both sets (training: area under the curve (AUC) 0.836 and testing: AUC, 0.817). When combined with CT-reported tumor status, the radiomics model demonstrated excellent calibration and discrimination, achieving an AUC of 0.849 in the training set and 0.851 in the testing set. The radiomics model, incorporating both the radiomics signature and the CT-reported tumor status, could help in the preoperative individualized prediction of LN metastasis in male patients with RPUC.

Keywords

Renal pelvis urothelial carcinoma; Radiomics; Lymph node metastasis; Computed tomography; Men

1. Background

Renal pelvis urothelial carcinoma (RPUC) is an uncommon condition, accounting for 5% to 10% of all diagnosed urothelial cancers, with a higher occurrence in men (male:female ratio = 2:1) [1]. In China, urothelial carcinoma incidence from the renal pelvis and ureters is notably higher, ranging from 20% to 30%, surpassing rates observed in Western countries [2]. Recent research reports male gender as an independent risk factor associated with RPUC [3]. In the last twenty years, the percentage of male patients with RPUC has steadily risen, and these patients notably face a lower cancer-specific survival rate compared to female patients. The recurrence and mortality rates associated with RPUC in male patients have gained increased attention among clinicians. The unusual presentation of this condition makes it difficult to gather sufficient evidence for risk stratification to guide therapeutic choices [4]. In recent years, collaborative efforts across multiple institutions have improved our understanding of crucial prognostic variables and the natural course of the disease.

Pelvic lymph node dissection (LND) is considered an important element in the surgical treatment of urothelial bladder cancer [5]. While it assists in postoperative risk assessment and potentially enhances patient survival, definitive evidence supporting these advantages is yet to be established through prospective trials [6]. In contrast, the significance of LND in those undergoing radical nephroureterectomy (RNU) for RPUC is still debatable partly due to its low incidence. Nevertheless, it is essential to recognize that LND plays a significant role in the prognostic management of patients already diagnosed with LN metastasis (LNM) [7]. Therefore, early confirmation of preoperative LNM in male RPUC patients are of great importance for guiding subsequent treatment and assessing prognosis.

Computed tomography (CT) plays a vital role as a non-invasive, rapid and precise imaging technique, establishing itself as a critical diagnostic tool for urothelial carcinoma. CT imaging enables the visualization of urothelial cancer, providing valuable information regarding its location, extent, depth of invasion, and potential detection of LNM in patients

[8]. Despite its effectiveness, CT imaging has limitations, as it cannot directly reveal details within small LN metastases, which may lead to potential false-negative results [9]. Additionally, the widespread distribution of LNs presents challenges for the detection of metastases using conventional CT [10]. In recent years, the emerging field of radiomics has harnessed advanced technologies, such as big data mining, to extract subtle quantitative features from medical images that are imperceptible to the naked eye. Through the analysis of the correlation between image features and clinical data, radiomics establishes predictive models for diseases, providing robust decision-support tools in the field of oncology [11]. Currently, significant progress has been made in radiomics for predicting tumor LNM across various cancers, including breast cancer [12], rectal cancer [13], liver cancer [14], lung cancer [15], and others. However, it is worth noting that there have been no reported findings related to RPUC in this context.

Therefore, we utilize CT images to extract radiomics features strongly associated with LNM, identify radiomics markers and, ultimately, integrate them with clinical features to develop a comprehensive model for estimating the LNM in male patients with RPUC.

2. Materials and methods

2.1 General information

We retrospectively analyzed the data of 133 male patients diagnosed with RPUC from 2018 to 2022 in the surgical database of the urology department. Inclusion criteria comprised: (1) initial postoperative pathological confirmation of RPUC in male patients, (2) urography performed within 20 days prior to surgery, and (3) acceptable quality of enhanced CT images. Exclusion criteria comprised: (1) the presence of prior or concurrent malignancies, (2) presence of imaging artifacts complicating cancer segmentation, and (3) absence of clinical data. Patient stratification into training ($n = 94$) and testing ($n = 39$) cohorts was based on treatment time, specifically from February 2018 to April 2020 and from May 2020 to June 2022.

2.2 CT image acquisition and LN status

Patients underwent multiple CT scans using a Somatom Definition 40 (Siemens Medical Systems) with parameters: 120 kV, 200 effective mAs, 64×0.6 mm beam collimation, 512×512 matrix, 0.8 pitch, and 0.5 s gantry rotation. Post non-enhanced scanning, dynamic contrast-enhanced scans were done at 25–30 s (arterial phase) and 60 s (portal phase) following 1.0 mL/kg iodinated contrast (Ultravist 370, Bayer Schering Pharma, Berlin-Wedding, Germany) injection at 2.0 mL/s into the antecubital vein. Two experienced urological radiologists (10 and 15 years) reviewed the CT images, noting T staging and LN sizes. Pelvic LNs over 8 mm and abdominal LNs over 10 mm were deemed clinically LN-positive [1]. Disagreements were resolved through consultation. Pathological staging used the 2009 tumor node metastasis (TNM) system [4], and grading followed the 2004 World Health Organization classification [5].

2.3 Feature selection and radiomics signature building

We outlined the region of interest (ROI) of the whole tumor on the arterial-phase CT imaging's largest cross-section. The segmented tumor ROI files were then transferred to Analysis Kit software (V3.0.2., Workbench2014, GE Healthcare, Chicago, IL, USA) for radiomics evaluation. The py-Radiomics Library (version 2.1.1) within AK was utilized to extract 960 radiomics features. To normalize these features for comparability, they were standardized, ensuring consistent evaluation across different units and scales. Feature dimensionality reduction was conducted using analysis of variance (ANOVA) and Mann-Whitney U-test (MW), complemented by correlation assessments using a Spearman coefficient of 0.9. The least absolute shrinkage and selection operator (LASSO) was then applied to pinpoint the most predictive features. These features, weighed by their coefficients, were linearly combined to form a radiomics score (Rad-score) for each patient, indicative of their risk of lymph node metastasis. The radiomics signature's accuracy was evaluated using the area under the receiver operating characteristic (ROC) curve in both sets.

2.4 Establishment of the radiomics nomogram

Using the training set, each potential predictor (*i.e.*, age, tumor size, tumor region, CT-reported number of tumors, CT-reported LN status, and Rad-score) was analyzed for its correlation with pathological lymph node metastasis using univariate logistic regression. Variables significant in this analysis ($p < 0.05$) were considered for the multivariate logistic model. The model's variable selection was further refined using bootstrap resampling (500 iterations). Predictors consistently significant in over 50% of these iterations were included in the final model. This model's performance was represented as a nomogram and evaluated for discrimination and fit using ROC techniques and the Hosmer-Lemeshow test. Additionally, a calibration curve was used to compare actual versus predicted LNM rates. These evaluation methods were applied to both the training and testing sets.

2.5 Statistical analysis

Statistical analyses were performed using various programs: MedCalc (V.11.2, 2011 MedCalc Software bvba, Mariakerke, Belgium), SPSS version 22.0 (IBM, Armonk, NY, USA), GraphPad (V3.10, GraphPad Software, San Diego, CA, USA), and R software (version 3.4.1; <http://www.r-project.org/>). The normality of variable distributions was evaluated using the Kolmogorov-Smirnov test. Depending on their distribution, continuous variables were analyzed using either two-sample *t*-tests or Mann-Whitney U tests, while categorical variables were assessed with Chi-square tests. All statistical tests were two-sided with a significance threshold set at $p < 0.05$.

3. Results

3.1 Baseline characteristics of the study cohort

The patient characteristics in both sets are summarized in Tables 1 and 2, respectively. Notably, a significant difference in CT-reported T stage was observed between patients with and without LNM in both the training and testing sets ($p < 0.05$). However, there were no significant differences in other variables ($p > 0.05$). In the training set, patients with pathological lymph node (pN) 1–3 constituted 37.23% (35/94), while in the testing set, this percentage was 35.89% (14/39). Importantly, among all patients, 48.98% (24/49) were not initially reported to have LNM but were found to have pathological LN metastases upon further examination. Conversely, 24.06% (32/133) of patients were initially reported to have LN metastases but did not exhibit LN metastases on pathological evaluation.

TABLE 1. Clinical characteristics of the training and testing sets.

Variable	Training set (n = 94)		Testing set (n = 39)		p value
	n	%	n	%	
Age	64.5 ± 10.8		64.3 ± 10.6		0.913
Tumor size					
<3 cm	49	52.1	23	59.0	0.596
>3 cm	45	47.9	16	41.0	
Region					
Left	66	70.2	28	71.8	0.855
Right	28	29.8	11	28.2	
CT-reported number of tumors					
Single	63	67.0	22	56.4	0.336
Multiple	31	33.0	17	43.6	
CT-reported T stage					
cT0–2	48	51.1	19	48.7	0.955
cT3–4	46	48.9	20	51.3	
CT-reported LN status					
cN0	41	43.6	13	33.3	0.365
cN1–3	53	56.4	26	66.7	

CT: computed tomography; LN: lymph node.

3.2 Construction and validation of radiomics signatures

Based on the ROI area on the arterial-phase CT scans 960 texture features were retrieved. After conducting single-factor ANOVA and Mann-Whitney tests, 265 of the initial 960 features were identified as potential features for further analysis. Subsequently, correlation test identified 68 features for further consideration. To establish the final composition of the most valuable predictive feature set, a LASSO logistic regression model was used, which identified eight valuable predictive features (Fig. 1). The radiomics signature, based on these eight features, demonstrated significantly different radiomics scores

between the pN0 (-0.439 ± 1.511) and pN1–3 (1.159 ± 0.689) patient subgroups in the training set ($p < 0.05$), which was validated using the testing set (pN0 (-0.07 ± 1.298), pN1–3 (1.15 ± 0.761), $p < 0.05$). The radiomics signature showed promising predictive capability, achieving an area under the curve (AUC) of 0.836 (95% confidence interval (CI), 0.748–0.924) (sensitivity and specificity: 0.915 and 0.657) in the training set and 0.817 (95% CI, 0.666–0.969) (sensitivity and specificity: 0.760 and 0.857) in the testing set.

3.3 Radiomics model performance

Univariate analyses revealed that CT-reported T stage and LN status, along with our derived radiomics signature, were associated with LNM in RPUC (Table 3). Subsequently, a radiomics model was constructed using multivariate logistic regression, incorporating these two predictors. The Hosmer-Lemeshow test confirmed the absence of overfitting in the model ($p > 0.05$). The calibration curve showed the model's predictive performance closely aligned with actual LNM status. It reached a predictive accuracy of 0.849 (95% CI, 0.761–0.915) in the training set, as per its AUC. In the testing set, the model's AUC was 0.851 (95% CI, 0.701–0.945), with sensitivities of 0.881 and 0.920, and specificities of 0.743 and 0.714 in the training and testing sets, respectively (Fig. 2).

3.4 Clinical evaluation of radiomics model

To assess prediction performance, we generated ROC curves using the 133 patient data, comparing the radiomics model, radiomics signature, and conventional CT-assessed T stage (Fig. 3A). The AUCs for the radiomics model, radiomics signature, and conventional CT-assessed T stage were 0.848 (95% CI, 0.776–0.904), 0.829 (95% CI, 0.754–0.889), and 0.634 (95% CI, 0.546–0.716), respectively. The radiomics model demonstrated superior predictive ability compared to either the radiomics signature or the CT-reported LN status alone in predicting pathological LN metastases. Furthermore, the radiomics model exhibited robust discriminatory performance within the cN0 subgroup, achieving an AUC of 0.903 (95% CI, 0.792–0.967) (Fig. 3B). Risk scores generated from the model allowed for classifying patients into low-risk and high-risk groups using optimal cut-off values set at 0.63887, identified through the maximum Youden index in the training set. Analysis revealed that both in the overall patient cohort and the cN0 subgroup, the high-risk group showed a significantly higher probability of LNM compared to the low-risk group (Fig. 3C,D).

4. Discussion

The results of this study highlight the effectiveness of the radiomics label marker, constructed based on the radiomic characteristics of the primary lesion in RPUC, in accurately determining the status of LNM. Importantly, the incorporation of the T-grade feature from clinical CT reports substantially improves predictive performance, emphasizing the clinical utility of radiomics characteristics, especially when combined with clinical tumor T staging, as a convenient and rapid diagnostic tool to estimate LNM in male RPUC patients.

TABLE 2. Clinical characteristics of the training and testing sets for pathological lymph node stage.

Variable	Training set (n = 94)			Testing set (n = 39)		
Pathologic T stage	pN1–3 (n = 35)	pN0 (n = 59)	<i>p</i>	pN1–3 (n = 14)	pN0 (n = 25)	<i>p</i>
	n (%)	n (%)		n (%)	n (%)	
Age	62.4 ± 11.1	65.4 ± 10.2	0.192	63.6 ± 13.6	65.0 ± 9.2	0.695
Tumor size						
<3 cm	18 (51.4)	31 (52.5)	0.741	8 (57.1)	15 (60.0)	0.862
>3 cm	17 (48.6)	28 (47.5)		6 (42.9)	10 (40.0)	
Region						
Left	27 (77.1)	39 (66.1)	0.369	10 (71.4)	18 (72.0)	0.970
Right	8 (22.9)	20 (33.9)		4 (28.6)	7 (28.0)	
CT-reported number of tumors						
Single	22 (62.9)	41 (69.5)	0.664	8 (57.1)	14 (56.0)	0.945
Multiple	13 (37.1)	18 (30.5)		6 (42.9)	11 (44.0)	
CT-reported T stage						
cT0–2	23 (65.7)	25 (42.4)	0.048	10 (71.4)	9 (36.0)	0.074
cT3–4	12 (34.3)	34 (57.6)		4 (28.6)	16 (64.0)	
CT-reported LN status						
cN0	22 (62.9)	41 (69.5)	0.664	2 (14.3)	11 (44.0)	0.125
cN1–3	13 (37.1)	18 (30.5)		12 (85.7)	14 (56.0)	

CT: computed tomography; LN: lymph node; pN: pathological lymph node.

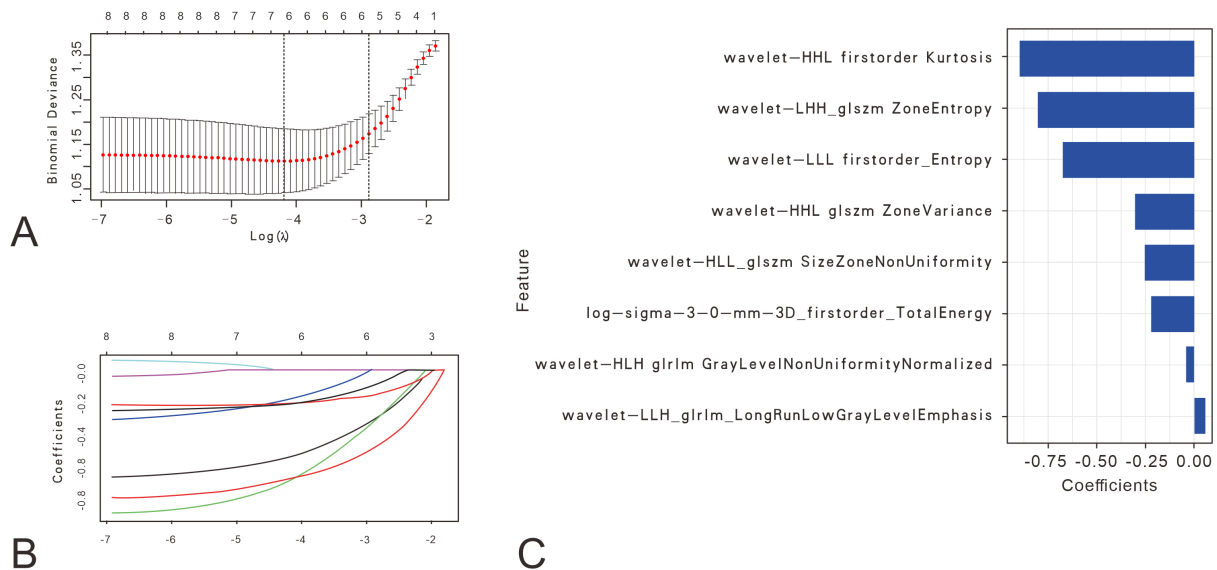


FIGURE 1. Radiomics features identified by the LASSO logistic regression method. (A) Radiomics feature selection using LASSO logistic regression. (B) LASSO coefficient profiles of the 68 texture features. (C) A vertical line was drawn at the value selected using 10-fold cross-validation in the $\log(\lambda)$ sequence, indicating ten coefficients with non-zero values.

TABLE 3. Logistic regression analyses of predicting pathological lymph node metastases.

Variable	Univariate logistic regression		Multivariate logistic regression	
	OR (95% CI)	<i>p</i>	OR (95% CI)	<i>p</i>
Age (<60 yr vs. >60 yr)	0.470 (0.144–1.536)	0.211	NA	NA
Tumor size (<3 cm vs. >3 cm)	0.672 (0.210–2.149)	0.502	NA	NA
CT-reported number of tumors (single vs. multiple)	1.920 (0.526–7.002)	0.323	NA	NA
CT-reported T stage (cT0–2 vs. cT3–4)	0.261 (0.072–0.947)	0.041	0.058 (0.008–0.396)	0.004
CT-reported LN status (cN0–cN1–3)	0.132 (0.028–0.621)	0.010	NA	NA
The radiomics signature (per 0.1 increase)	0.130 (0.044–0.385)	<0.001	0.085 (0.013–0.546)	0.009

Note: NA, not available. These variables were eliminated in the multivariate logistic regression model, so the OR and *p* values were not available. CT: computed tomography; LN: lymph node; CI: confidence interval; OR: odds ratio.

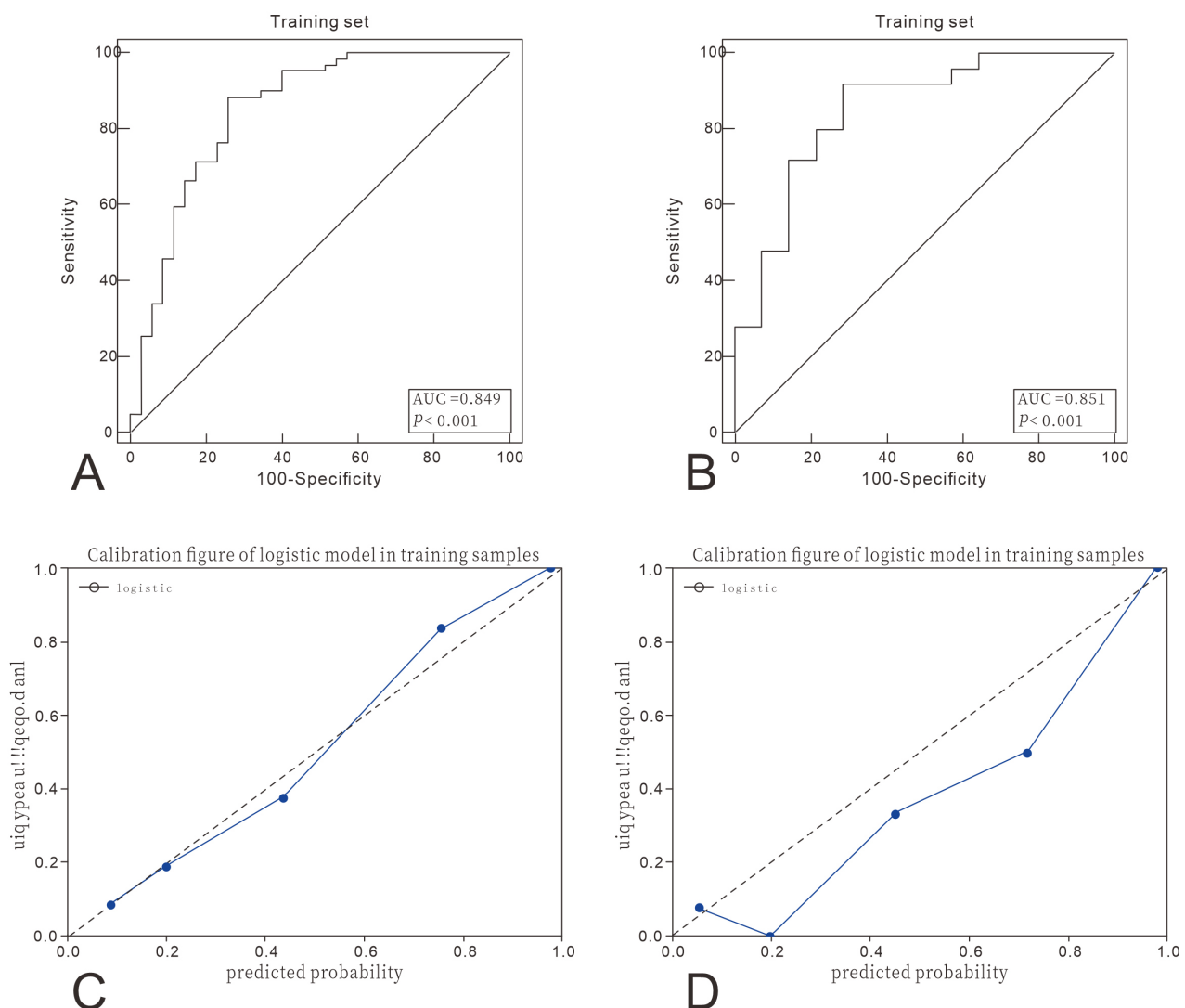


FIGURE 2. The ROC curves and calibration curves of the radiomics model. (A) The ROC curve of the radiomics model in the training group. (B) The ROC curve of the radiomics model in the testing group. (C) The calibration curve of the radiomics model in the training group. (D) The calibration curve of the radiomics model in the testing group. AUC: area under the curve.

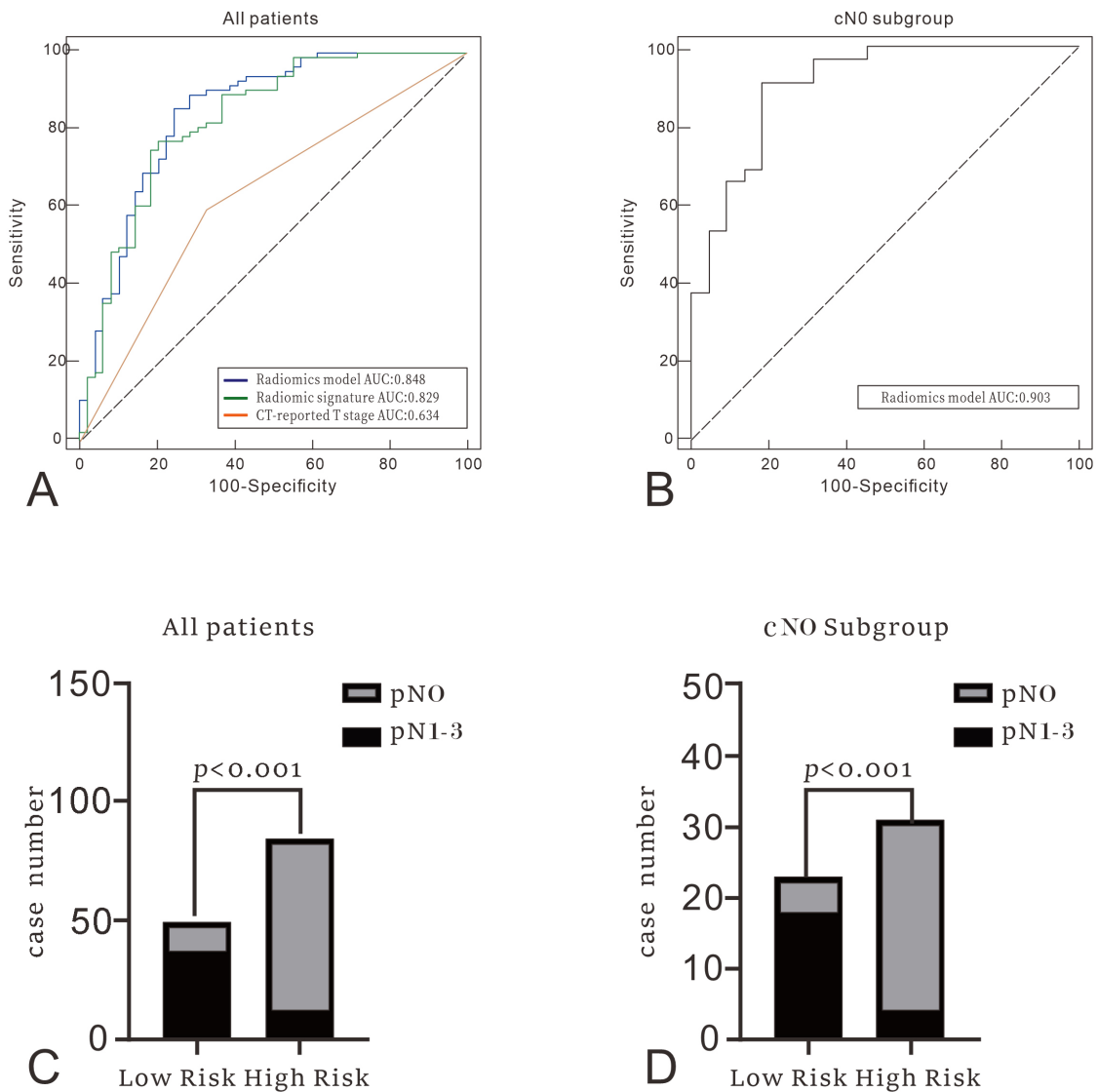


FIGURE 3. Clinical evaluation of radiomics model in all patients and cN0 subgroup. (A) The ROC curves of on all 133 patients were plotted for the radiomics model, radiomics signature, and conventional CT-assessed T stage. (B) The AUC of the model for predicting pathological lymph node metastases in the cN0 subgroup. (C) The model's efficacy in identifying LNM in the high-risk group and low-risk group in all patients. (D) The model's efficacy in identifying LNM in the high-risk group and low-risk group in cN0 subgroup. AUC: area under the curve; CT: computed tomography; pN: pathological lymph node.

LNM significantly influences treatment decisions, prognosis assessment and the prognosis of RPUC [16]. Effective predictive models are necessary for guiding treatment choices and improving patient outcomes. For instance, in surgical procedures, predictive outcomes can inform decisions regarding LN dissection and postoperative chemotherapy, thereby reducing surgical risks and enhancing survival rates. In regards to radiotherapy and chemotherapy, adjusting treatment regimens and doses based on predictive outcomes can optimize treatment effectiveness while minimizing adverse effects. The results of this study demonstrate that the developed radiomics model, which integrates tumor radiomics markers with clinical tumor T staging, effectively predicts LNM in RPUC, which has substantial implications for advancing the application of

radiomics in both RPUC research and clinical practice. Tumor T stage, a crucial component of the constructed model, has been established as significantly associated with RPUC patient survival [17]. In line with the findings of Seisen *et al.* [18] and Cha *et al.* [19], a more advanced T stage was identified as a promising risk factor linked to patient survival. The present study aligns with this conclusion, as only T stage was incorporated in the radiomics model construction, further highlighting the potential association between LNM and patient prognosis. However, it is essential to acknowledge that the clinical T stage may not consistently serve as an independent predictor of RPUC pathological characteristics in similar studies [20], possibly due to variations in the sizes of the study populations. Thus, future investigations should consider larger sample sizes

to validate the findings of this study.

In our study, we used the constructed radiomics model to predict the risk for all male patients, and based on these risk data, patients were categorized into either high-risk or low-risk groups. Notably, the study revealed a significantly higher detection rate of pathological LN-positive patients in the high-risk group compared to the low-risk group, which underscores the clinical superiority of the radiomics model over serological testing as a prognostic tool for RPUC [21]. Furthermore, our use of models to predict outcomes in patients initially classified as having negative LNs based on clinical CT reports not only exhibited good diagnostic accuracy but also demonstrated the ability to differentiate between high and low risk, suggesting that the radiomics model may serve as a reliable non-invasive biomarker for accurately diagnosing the absence of LNM in RPUC patients through clinical imaging. While urine cytology has been considered a non-invasive marker for RPUC prognosis, its accuracy is significantly limited by a high false-negative rate, which can reach up to 50 percent in low-grade tumors [22].

However, it is important to acknowledge several limitations in this study. Firstly, as a cross-sectional study conducted at only one center which had few cases analyzed. Future studies should prioritize larger data collection, incorporating multi-center datasets to enhance the accuracy and reliability of predictive models. Secondly, this study relied on a single image feature report, lacking the integration of diverse imaging and clinical data. Subsequent research should aim to construct a more intricate and comprehensive prediction model, thereby improving predictive performance and expanding the application scope. Lastly, this study did not investigate the correlation of the factors with LNM in RPUC and associated radiomics features. Such an investigation could provide valuable insights into the explanatory and biological significance of predictive models.

5. Conclusions

In summary, our proposed model constructed for estimating RPUC LNM shows promising potential for clinical application. However, further research is warranted to validate our findings, which could help radiomics evolve into a crucial tool for diagnosing and treating RPUC, providing male patients with more personalized, accurate and effective medical services.

AVAILABILITY OF DATA AND MATERIALS

The data presented in this study are available on reasonable request from the corresponding author.

AUTHOR CONTRIBUTIONS

JYH and CCG—designed the research study. JYH—performed the research. FC and GT—provided help and advice on the radiomics model. ZYS—analyzed the data. JYH, CCG and GT—wrote the manuscript. All authors contributed to editorial changes in the manuscript. All authors

read and approved the final manuscript.

ETHICS APPROVAL AND CONSENT TO PARTICIPATE

This study involving human participants was reviewed and approved by the Medical Research Ethics Committee of the Zhejiang Provincial People's Hospital, Affiliated People's Hospital, Hangzhou Medical College, Hangzhou, China (NO. QT2022422). Written informed consent was provided by the participants' legal guardians or next of kin.

ACKNOWLEDGMENT

We express our gratitude to all the patients for their cooperation and willingness to participate in this study.

FUNDING

This research received no external funding.

CONFLICT OF INTEREST

The authors declare no conflict of interest.

REFERENCES

- [1] Soria F, Shariat SF, Lerner SP, Fritsche H, Rink M, Kassouf W, *et al.* Epidemiology, diagnosis, preoperative evaluation and prognostic assessment of upper-tract urothelial carcinoma (UTUC). *World Journal of Urology.* 2017; 35: 379–387.
- [2] Wu J, Chen S, Wu X, Mao W, Wang Y, Xu B, *et al.* Trends of incidence and prognosis of upper tract urothelial carcinoma. *Bosnian Journal of Basic Medical Sciences.* 2021; 21: 607–619.
- [3] Xu C, Yuan C, Zhang C, Fang D, Yu Y, Wang X, *et al.* The evolution of clinicopathological diagnostic features of upper tract urothelial carcinoma in China: a summary of 2561 cases in the last 20 years. *Frontiers in Oncology.* 2022; 12: 769252.
- [4] Califano G, Ouzaid I, Verze P, Hermieu J, Mirone V, Xylinas E. Immune checkpoint inhibition in upper tract urothelial carcinoma. *World Journal of Urology.* 2021; 39: 1357–1367.
- [5] Rouprêt M, Babjuk M, Burger M, Capoun O, Cohen D, Compérat EM, *et al.* European association of urology guidelines on upper urinary tract urothelial carcinoma: 2020 update. *European Urology.* 2021; 79: 62–79.
- [6] Voskuilen CS, Schweitzer D, Jensen JB, Nielsen AM, Joniau S, Muilwijk T, *et al.* Diagnostic value of 18F-fluorodeoxyglucose positron emission tomography with computed tomography for lymph node staging in patients with upper tract urothelial carcinoma. *European Urology Oncology.* 2020; 3: 73–79.
- [7] Pallauf M, D'Andrea D, König F, Laukhtina E, Yanagisawa T, Rouprêt M, *et al.* Diagnostic accuracy of clinical lymph node staging for upper tract urothelial cancer patients: a multicenter, retrospective, observational study. *Journal of Urology.* 2023; 209: 515–524.
- [8] Rodler S, Solyanik O, Ingenerf M, Fabritius M, Schulz GB, Jokisch F, *et al.* Accuracy and prognostic value of radiological lymph node features in variant histologies of bladder cancer. *World Journal of Urology.* 2022; 40: 1707–1714.
- [9] Dłubak A, Karwacki J, Logoń K, Tomecka P, Brawańska K, Krajewski W, *et al.* Lymph node dissection in upper tract urothelial carcinoma: current status and future perspectives. *Current Oncology Reports.* 2023; 25: 1327–1344.
- [10] Richters A, van Ginkel N, Meijer RP, Wondergem M, Schoots I, Vis AN, *et al.* Staging fluorodeoxyglucose positron emission tomography/computed tomography for muscle-invasive bladder cancer: a

- nationwide population-based study. *BJU International*. 2023; 132: 420–427.
- [11] Amudala Puchakayala PR, Sthanam VL, Nakhmani A, Chaudhary MFA, Kizhakke Puliyakote A, Reinhardt JM, *et al*. Radiomics for improved detection of chronic obstructive pulmonary disease in low-dose and standard-dose chest CT scans. *Radiology*. 2023; 307: e222998.
- [12] Ramtohul T, Djerroudi L, Lissavalid E, Nhy C, Redon L, Ikni L, *et al*. Multiparametric MRI and radiomics for the prediction of HER2-zero, -low, and -positive breast cancers. *Radiology*. 2023; 308: e222646.
- [13] Shin J, Seo N, Baek S, Son N, Lim JS, Kim NK, *et al*. MRI radiomics model predicts pathologic complete response of rectal cancer following chemoradiotherapy. *Radiology*. 2022; 303: 351–358.
- [14] Carbonell G, Kennedy P, Bane O, Kirmani A, El Homsi M, Stocker D, *et al*. Precision of MRI radiomics features in the liver and hepatocellular carcinoma. *European Radiology*. 2022; 32: 2030–2040.
- [15] Chetan MR, Gleeson FV. Radiomics in predicting treatment response in non-small-cell lung cancer: current status, challenges and future perspectives. *European Radiology*. 2021; 31: 1049–1058.
- [16] Kobayashi S, Ito M, Takemura K, Suzuki H, Yonese I, Koga F. Preoperative models incorporating the systemic immune-inflammation index for predicting prognosis and muscle invasion in patients with non-metastatic upper tract urothelial carcinoma. *International Journal of Clinical Oncology*. 2022; 27: 574–584.
- [17] Aydh A, Abufaraj M, Mori K, Quhal F, Pradere B, Motlagh RS, *et al*. Performance of fluoro-2-deoxy-D-glucose positron emission tomography-computed tomography imaging for lymph node staging in bladder and upper tract urothelial carcinoma: a systematic review. *Arab Journal of Urology*. 2021; 19: 59–66.
- [18] Seisen T, Colin P, Hupertan V, Yates DR, Xylinas E, Nison L, *et al*. Postoperative nomogram to predict cancer-specific survival after radical nephroureterectomy in patients with localised and/or locally advanced upper tract urothelial carcinoma without metastasis. *BJU International*. 2014; 114: 733–740.
- [19] Cha EK, Shariat SF, Kormaksson M, Novara G, Chromecki TF, Scherr DS, *et al*. Predicting clinical outcomes after radical nephroureterectomy for upper tract urothelial carcinoma. *European urology*. 2012; 818–825.
- [20] Sugino Y, Sasaki T, Kato M, Masui S, Nishikawa K, Okamoto T, *et al*. Prognostic effect of preoperative psoas muscle Hounsfield unit at radical cystectomy for bladder cancer. *Cancers*. 2021; 13: 5629.
- [21] Miura N, Mori K, Laukhtina E, Schuetthfort VM, Abufaraj M, Teoh JYC, *et al*. Prognostic value of the preoperative albumin-globulin ratio in patients with upper urinary tract urothelial carcinoma treated with radical nephroureterectomy: results from a large multicenter international collaboration. *Japanese Journal of Clinical Oncology*. 2021; 51: 1149–1157.
- [22] Tanaka N, Kikuchi E, Kanao K, Matsumoto K, Shirotake S, Kobayashi H, *et al*. The predictive value of positive urine cytology for outcomes following radical nephroureterectomy in patients with primary upper tract urothelial carcinoma: a multi-institutional study. *Urologic Oncology*. 2014; 32: 48.e19–48.e26.

How to cite this article: Jingyi Huang, Fan Chen, Chengcheng Gao, Zhenyu Shu, Gang Tao. A radiomics model derived by combination of radiomics signature and clinical risk factors predict of lymph node metastasis for men renal pelvis urothelial carcinoma. *Journal of Men's Health*. 2024; 20(5): 68-75. doi: 10.22514/jomh.2024.072.